AIAA JOURNAL
Vol. 44, No. 10, October 2006

Control of Laminar Separation Bubbles Using Instability Waves

Ulrich Rist* and Kai Augustin†
Universität Stuttgart, 70550 Stuttgart, Germany

DOI: 10.2514/1.17518

This paper presents detailed investigations related to active transition control in laminar separation bubbles. The investigations rely on direct numerical simulations based on the complete Navier–Stokes equations for a flat-plate boundary layer. A laminar separation bubble is created by imposing a streamwise adverse pressure gradient at the freestream boundary of the integration domain. Different steady and unsteady boundary layer disturbances are then introduced at a disturbance strip upstream of separation and their effects on the separation bubble are studied. It is shown that the size of the separated region can be controlled most efficiently by very small periodic oscillations, which lead to traveling instability waves that grow to large levels by the hydrodynamic instability of the flow. Indications for the preferred frequency of these waves can be obtained from linear stability theory, but since the problem is nonlinear, only direct numerical simulations can really qualify or disqualify the predictions. Overall, it turns out that unsteady two- or three-dimensional disturbances have a stronger impact on the size of the bubble than steady disturbances, because they directly provide initial amplitudes for the laminar-turbulent transition mechanism.

Nomenclature

f	=	disturbance frequency
$H = \delta^*/\Theta$	=	shape parameter
(h/k)	=	mode of the frequency (index h) spanwise wave number spectrum (index k)
L	=	reference length
R	=	reattachment point
$Re^* = U_\infty \delta^*/\upsilon$	=	displacement-thickness Reynolds number
$Re_\Theta = U_\infty \Theta/\upsilon$	=	momentum-thickness Reynolds number
S	=	separation point
T	=	laminar-turbulent transition
U_M	=	mean velocity at the freestream boundary of the integration domain
U_P	=	potential velocity prescribed at the freestream boundary
U_∞	=	freestream velocity
v'	=	wall-normal disturbance amplitude at the wall
x	=	streamwise coordinate
y	=	wall-normal coordinate
z	=	spanwise coordinate
α	=	streamwise wave number
α_T	=	spreading angle of turbulence (conceptual)
$\beta = 2\pi f L/U_\infty$	=	nondimensional disturbance frequency
δ^*	=	displacement thickness
Θ	=	momentum thickness
ϕ	=	obliqueness angle of traveling waves (with respect to the x axis)
ω_z	=	spanwise vorticity

I. Introduction

THE occurrence of laminar separation and turbulent reattachment in a so-called laminar or transitional separation bubble is a typical problem for low to medium Reynolds-number aerodynamics, for example, on aircraft wings or blades of turbo machines, where they lead to unwanted performance penalties. Laminar separation bubbles should hence be avoided using some means of control. So far, this has been achieved primarily by a "cautious" design or by placing some kind of turbulence trips or vortex generators upstream of separation [1]. However, these approaches cannot adapt themselves to changing operation conditions such that performance penalties may occur under off-design conditions. On the other hand, avoiding laminar separation bubbles by design sacrifices the maximal possible efficiency or adds extra weight and costs to a turbine because of extra blades which are needed to make the passage narrower in order to keep the flow attached.

Therefore, more advanced active systems which generate oscillations to control separation by either applying periodic suction and blowing via synthetic jets using piezoelectric actuators, some kind of micro-electro-mechanical systems (MEMS), or aerodynamic flow control have been used successfully to control laminar and turbulent separation [2,3]. An excellent review of separation control using periodic excitation can be found in Greenblatt and Wygnanski [4], for instance. Another approach for active control is to periodically deform the otherwise smooth surface layer of an airfoil. Sinha [5] suggests a system using active flexible-wall transducers to control separated flow from the vicinity of the separation by so-called "micro-flexural wall vibrations" combining sensors and actuators. Applied to a laminar flow, which is very sensitive to surface roughness, such a system would not induce additional drag when switched off. As a drawback, such systems only provide very small deformation amplitudes, in order to be low energy consuming, and imply electric driving and control devices. But such surface-bound active devices could generate the necessary high-frequency perturbations to excite shear-layer instabilities that promote an earlier laminar-turbulent transition.

In low-pressure turbines, to name another area of potential application for the present research, active separation control methods have also been proposed recently. Mostly, they consist of using vortex generator jets (e.g., Bons et al. [6]) which enforce an earlier transition of the flow to turbulence and hence an earlier reattachment or no laminar separation at all using brute force. More recently periodically pulsed jets have been found to increase the efficiency of such devices [7]. On the other hand, detailed low-pressure turbine cascade measurements have shown that laminar separation bubbles which periodically disappear and reappear under the influence of periodically passing wakes exert less dissipation loss on the cascade compared with the fully turbulent case. According to Stieger and Hodson [8], this is due to periodically appearing "calmed regions" after destruction of the laminar separation bubble (LSB) by the passage of a turbulent wake, before the LSB reappears. Such findings

Received 6 May 2005; revision received 13 April 2006; accepted for publication 14 April 2006.

*Außerplanmäßiger Professor, Institut für Aerodynamik und Gasdynamik, Pfaffenwaldring 21.

†Research Assistant, Institut für Aerodynamik und Gasdynamik; currently R&D Engineer, Behr GmbH & Co. KG, Siemensstrasse 164, 70469 Stuttgart, Germany.

confirm that active separation control has the potential to reduce dissipation losses in a low-pressure turbine environment, also.

In the present work we investigate the possibility of using small-amplitude, local wall vibrations or suction and blowing to excite low-amplitude Tollmien–Schlichting wave-like periodic boundary layer disturbances which are amplified by the hydrodynamic instability of the laminar boundary layer such that they control transition in a typical laminar separation bubble. Originally intended for laminar separation bubbles in aerodynamic boundary layers (i.e., along external surfaces, like a wing), our simulation results should be equally valid for boundary layers in turbo machines because of very similar boundary layer thicknesses and shape parameters.

II. Physical Mechanisms of a Transitional Laminar Separation Bubble

Laminar boundary layers are preferable for applications where a low skin friction is desired. However, they are very sensitive to adverse pressure gradients, and they tend to separate much earlier than a turbulent boundary layer. Thus, in a typical aerodynamic context with a changeover from favorable to adverse-pressure gradient, a region of laminar flow typically ends with a transitional LSB soon after the flow encounters the adverse-pressure gradient. The separated flow leads to uncontrolled unsteadiness and an additional pressure drag penalty. Both are difficult to predict because of the sensitivity of the flow to small background disturbances, which are usually unknown because they cannot be measured.

The basic setup of a LSB is sketched in Fig. 1. The laminar boundary layer separates from the wall at a point S, transition to turbulence takes place at T, and the turbulent flow reattaches at R.The latter occurs because of an increased momentum exchange normal to the wall under the action of the larger turbulence eddies. With some oversimplification the reattachment process can be thought to be due to a turbulent wedge that spreads at an angle α_T from a point in the detached shear layer. The actual transition process starts by amplification of small-amplitude disturbances, which are already present in the upstream laminar flow or which are ingested from the freestream via a process called "receptivity." Once large enough, higher frequencies occur and the shear layer disintegrates into structures of different size. For a more complete discussion of the laminar-turbulent transition process in LSBs see [9–12], for instance. Here, it is important to note that the position of T within the bubble strongly depends on the initial disturbances. Since R is related to the position of T and α_T, the bubble length (R–S) can be controlled by controlling the laminar-turbulent transition process, and it is the purpose of the present paper to present a detailed investigation of the underlying mechanisms. Therefore, the basic idea is to control laminar-turbulent transition by introducing small-amplitude disturbance waves upstream of the LSB. If these are in the unstable frequency range they will then grow to large amplitudes. The earlier they reach a certain level, the earlier laminar-turbulent transition and the earlier turbulent reattachment of the flow that closes the bubble. On the other hand, if laminar-turbulent transition happens too far away from the wall or if α_T is not large enough, the turbulent flow might not reattach to the wall which has drastic consequences on the pressure distribution (lift and drag). An active forcing of laminar-turbulent transition might also help to avoid such an "open separation."

The paper is organized as follows. First the used numerical method is presented. Then a base flow is selected out of those studied by Augustin [13]. The linear instability of this is shown next using linear stability theory (LST) and comparisons with direct numerical simulations (DNS), followed by a demonstration of the influence of different forcing frequencies and disturbance amplitudes on the size of the LSB. A section based on three-dimensional (3-D) simulations shows that obliquely traveling waves are an equally efficient means for control as two-dimensional (2-D) waves and that unsteady forcing is much more efficient than steady 3-D forcing, for example, via roughness elements. The paper ends with a summary and an outlook.

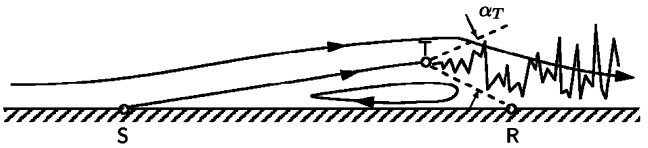

Fig. 1 Sketch of a transitional laminar separation bubble. S, T, and R: separation, transition, and reattachment, respectively

III. Numerical Method

To study laminar separation bubbles multiple DNS of a flat-plate boundary layer have been performed. An adverse-pressure gradient is applied locally at a given distance from the inflow at the freestream boundary to force separation. The code used for the present DNS has been developed, verified, and validated for the investigation of transitional boundary layers without and with separation [13–17].

Figure 2 displays a sketch of the used integration domain together with a definition of the coordinates and the respective velocity components. All variables are nondimensionalized with respect to U_∞ and L which leads to a reference Reynolds number given further down together with the results. The complete Navier–Stokes equations for incompressible flows are solved in a vorticity–velocity formulation [14]. A fourth-order accurate numerical method is applied in time and space by finite differences in streamwise and wall-normal direction and by a four step explicit Runge–Kutta scheme in time [16]. For the spanwise direction a Fourier series implying periodic boundary conditions in that direction is used. Because of this the Poisson equations for the streamwise and spanwise velocity reduce to ordinary differential equations. The remaining 2-D Poisson equation for the wall-normal velocity is solved by a line relaxation method accelerated by a nonlinear multigrid algorithm, once the vorticity–transport equations have been advanced to the next Runge–Kutta step [14]. All equations can be solved separately for each spanwise spectral mode k allowing effective parallelization.

At the inflow boundary a Blasius boundary layer solution with a displacement-thickness Reynolds number $Re^* = 1722$ is prescribed. At the surface of the plate the no-slip boundary condition is applied except for a disturbance strip upstream of the LSB where periodic 2-D and 3-D boundary-layer disturbances are introduced into the flow by suction and blowing. The streamwise length of the disturbance strip has been set to one wavelength of the most amplified disturbance mode according to LST and the beginning is located approximately two wavelengths downstream of the inflow boundary. For the total streamwise length of the integration domain 18.41 wavelengths have been used, and the height of the domain corresponds to 16 boundary layer displacement thicknesses at the inflow. The integration domain has been discretized with 2762 times 297 equidistant grid points in streamwise and wall-normal direction, respectively. One time period is resolved with 1000 time steps. To avoid nonphysical reflections at the outflow boundary the disturbance amplitudes are artificially damped in a buffer domain by several orders of magnitude, using the method described by Kloker et al. [15].

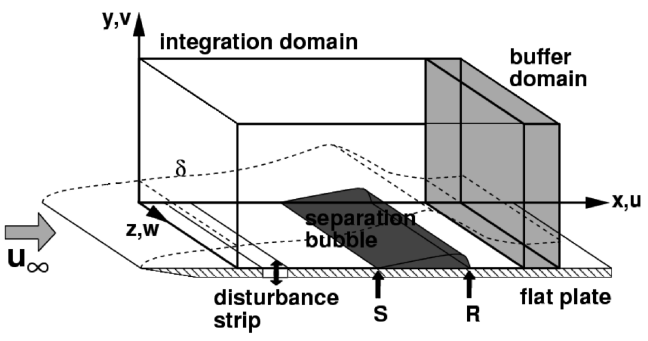

Fig. 2 Integration domain for DNS of LSB control.

The laminar separation bubble is induced by a local deceleration of the "potential" freestream velocity imposed via the u-component U_P at the upper boundary between $x = 10.86$ and $x = 16.39$. Because of Bernoulli's equation this corresponds to imposing an adverse pressure gradient. The displacement effects of the LSB on the potential flow are captured by a viscous–inviscid boundary-layer interaction model at every time step of the calculation [18,19]. The model changes the inviscid freestream velocity condition in accordance with the actual boundary-layer displacement thickness which is modeled by an equivalent source and sink distribution at the wall. Thus, the characteristic "pressure plateau" in the u-velocity distribution with a constant velocity in the upstream part of the separation bubble and a sharp velocity drop in the region of transition and reattachment develops during the calculation (see next section).

IV. Numerical Results

Three different streamwise velocity drops have been investigated [13]: one with 10%, one with 20%, and one with 25% reduction of freestream velocity, where 10% means a reduction from $U/U_\infty = 1$ to $U/U_\infty = 0.9$, for instance. A comparison of the three is performed in Fig. 3 in terms of the "potential velocity" U_P, the resulting velocity U_M at the freestream boundary, and in terms of the separation streamline $\Psi = 0$. (Note that the difference between U_M and U_P is the contribution of the viscous–inviscid interaction model.) Clearly, a larger velocity drop leads to a larger adverse-pressure gradient and hence earlier separation at the wall. Also, the height of the bubble increases with rising pressure gradient. In all cases the typical "pressure plateau" develops in the velocity U_M (thick lines) as a result of the implemented viscous–inviscid interaction [18]. Here and in the following, dimensions are normalized with respect to L and U_∞ which yields $Re = LU_\infty/\upsilon = 10^5$.

In the following, "case A" will be considered only, because LSB control works in a similar manner in all three cases [13], as well as in those studied already earlier [20,21].

A. Linear Instability of the Flow

Using velocity profiles $U(y)$ extracted at $x = \text{const}$ from the base flow obtained via DNS a linear stability analysis can be performed based on the Orr–Sommerfeld equation [22]. This analysis yields for a given x, Re, and frequency $\beta = 2\pi f L/U_\infty$, where f is the frequency in Hertz, a complex streamwise wave numbers α whose imaginary part α_i is called the amplification rate. Integrating α_i versus x for fixed β leads to the disturbance amplification ratio $A/A_0 = e^{-\int \alpha_i dx}$, where A_0 is the initial amplitude. Figure 4 presents results of such an analysis for base flow A and $A_0 = 10^{-6}$. The region of amplified disturbance frequencies is marked by increasingly dark shading. If the frequency is chosen correctly, for example, between $\beta = 2.5$ and $\beta = 5$ a dramatic amplitude increase by 10^4 is observed for the region shown. In contrast to what one might presume, the strong amplification starts well upstream of laminar separation (S) and is not just an indication of an inviscid "Kelvin–Helmholtz" instability. To make full use of these facts, the optimal disturbance generator placement should not be at the separation point but well upstream of this, that is, in the region $x < 12$ for the present case, which is also subject to the adverse-pressure gradient. As a rule, the actuator should not be placed in a region of favorable pressure gradient because the disturbances would be damped until they reach the adverse-pressure gradient. The optimum position is the station where amplification starts for the selected frequency (neutral point according to LST).

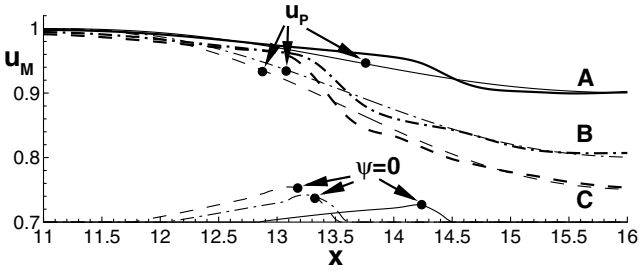

Fig. 3 Comparison of prescribed potential flow (thin lines) with resulting freestream velocity (thick lines) and separation streamlines for the three base flows with 10% (*A*, solid line), 20% (*B*, dash–dotted line), and 25% velocity drop (*C*, dashed line).

B. Verification in 2-D Simulations

The findings of the previous paragraph will now be checked using two-dimensional DNS. Primary parameters for the specification of 2-D disturbances at the upstream disturbance strip are the wall-normal suction and blowing amplitude v' (nondimensionalized with respect to U_∞) and the forcing frequency β. The range of amplified frequencies observed in Fig. 4 is rather narrow and should be obeyed for an efficient bubble control strategy, as already mentioned above. For the following simulations the frequency $\beta = 5$, indicated by the dashed line in Fig. 4, is chosen. A comparison of the obtained amplitude amplification with according LST results is shown in Fig. 5. The lines depict the maxima of the wall-parallel velocity disturbance component u' for the fundamental mode (1/0) and its higher harmonic (2/0), where (h/k) designates modes in the frequency (index h) spanwise wave number (index k) spectrum. The dash–dotted lines are results of LST for $\beta = 5$ and $\beta = 10$ (with symbols) shown for comparisons with and validation of the DNS. The excellent agreement between LST and DNS for the fundamental disturbance is most probably due to very large amplification in the laminar separation bubble, which is an order of magnitude larger than in an attached boundary layer such that differences due to nonparallel

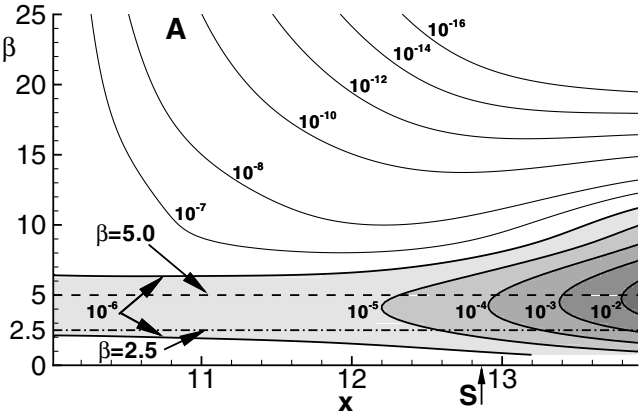

Fig. 4 Stability diagram for base-flow *A* according to linear stability theory.

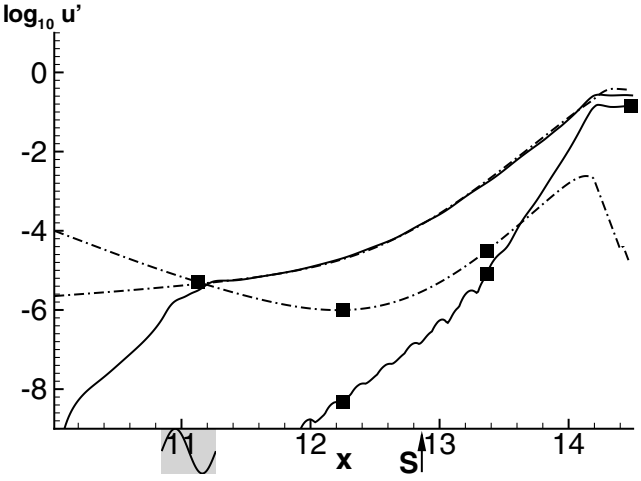

Fig. 5 Comparison of the growth of the fundamental disturbance (1/0) $\beta = 5$ and its first harmonic (2/0) $\beta = 10$ (marked with ■) with LST (dash–dotted lines).

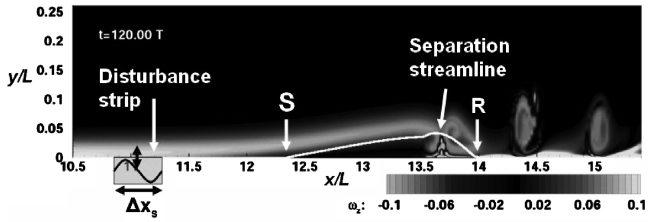

Fig. 6 Comparison of instantaneous vorticity with time-averaged separation streamline and placement of disturbance strip.

effects become negligibly small in logarithmic scale. Also, our pressure-induced bubbles are very shallow with separation angles around 1 deg.

Upstream of the disturbance strip (at $x \approx 11$) the fundamental disturbance amplitude decays to zero while the downstream growth corresponds over a large extent to the one predicted by LST. Since the higher harmonic is generated as a product of the fundamental with itself, it amplifies faster than its corresponding LST results (lines with squares). Overall, both disturbances grow over several orders of magnitude until nonlinear saturation which correlates with the formation of vortices discussed in connection with Fig. 6 further down. The constant-amplitude part of the fundamental and its higher harmonic correspond to vortex shedding in the rear part and downstream of the bubble and the point of nonlinear amplitude saturation corresponds to point T in the idealized sketch of Fig. 1.

Here, the reader should be reminded that laminar-turbulent transition and its influence on the laminar separation bubble are both nonlinear phenomena and that their prediction needs a full (nonlinear) simulation, that is, linear theory can give only a somewhat limited insight into the useful parameter range. It cannot predict laminar-turbulent transition and its impact on the bubble size. This is why the higher harmonic does not behave according to LST. In addition, once the bubble has become smaller the linear instability of the flow is somewhat reduced. Nevertheless, most of the disturbance growth follows linear instability closely and LST can be used to estimate the effect of choosing different forcing frequencies. In addition, LST helps to explain the initial mechanisms. Thus, the investigation of the *nonlinear* effects of unsteady forcing on the laminar separation bubble can so far only be investigated by full DNS.

As an illustration, results of one such simulation (frequency $\beta = 5$ and amplitude $v' = 10^{-6}$) are shown in Fig. 6 in terms of the instantaneous vorticity ω_z and the time-averaged separation streamline. The location and extent of the disturbance strip is again marked by a box at $x \approx 11.0$. The shear layer detaches from the surface at S and reattaches at R in the time mean. Downstream of the LSB a very high wall shear develops which resembles the high wall shear of a turbulent boundary layer despite the fact that only two-dimensional simulations have been performed here, and that a rather regular vortex shedding occurs in Fig. 6 due to the periodic forcing with a single frequency. It turned out that the wall-normal momentum transfer induced by these vortices has a similar effect on the time-averaged flow as if the flow became fully turbulent. For instance, the shape parameter of the present boundary layer after reattachment is close to $H = 2.0$ while the one for a turbulent boundary layer is $H = 1.4$–1.5. Inside the present bubble the shape factor rises to $H \approx 7$. Upstream of $x \approx 13$ the disturbances are too weak to be seen in Fig. 6. This is why a logarithmic scale has been used in Fig. 5.

C. Effect of Disturbance Frequency

Results of LST in Fig. 4 have indicated the frequency band necessary for an efficient control. Two possible discrete frequencies have been indicated by horizontal lines there. Figure 7 presents results for the lower disturbance frequency $\beta = 2.5$ in comparison with according LST results and the fundamental $\beta = 5$ from the previous case (dash–dotted line). A striking difference to Fig. 5 is that the higher harmonic ($\beta = 5$) lies also within the unstable region such that its growth agrees to an equally large extend with LST as the growth of the fundamental.

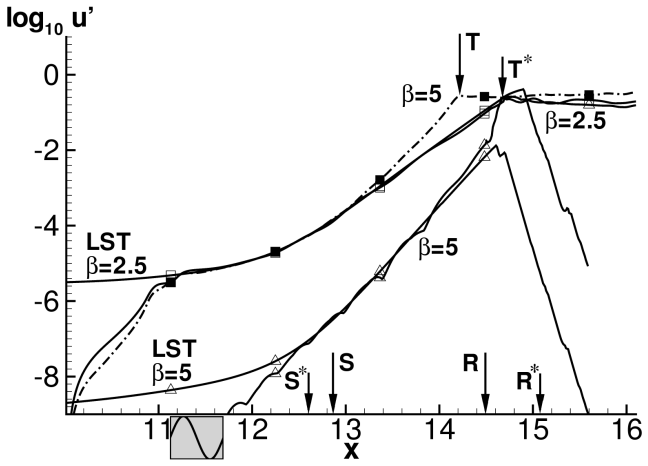

Fig. 7 Fundamental and higher harmonic disturbance growth for forcing with $\beta = 2.5$ compared with $\beta = 5$ (dash–dotted line) and LST. S^*, R^*, and T^* belong to the case with $\beta = 2.5$; R, S, and T to $\beta = 5$.

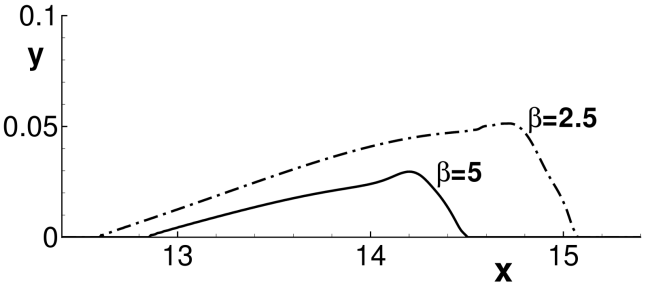

Fig. 8 Comparison of separation streamlines for forcing with $v' = 10^{-6}$ and two different frequencies.

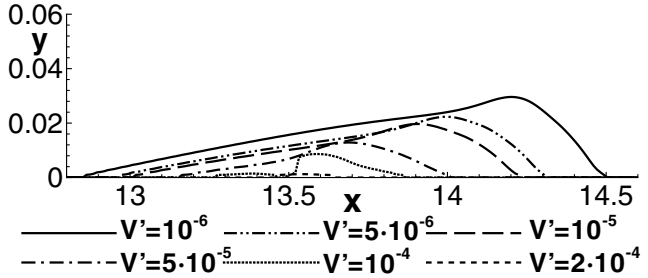

Fig. 9 Separation streamlines for increasing forcing amplitudes at frequency $\beta = 5$.

However, compared with the earlier case the fundamental of the present case (solid lines) grows somewhat slower after $x = 13$ such that nonlinear saturation of the disturbances (T^*) occurs farther downstream than in the first case (T). Since the position of reattachment is related to T, there is later reattachment (R^* at $x \approx 15$) compared with the first case (R), such that the laminar separation bubble becomes larger. Interestingly, the point of laminar separation moves upstream at the same time (S^* vs S), an effect already observed earlier [10].

Thus, despite the same forcing amplitude and identical initial growth of the disturbances in the two cases, bubbles of different size develop. This is emphasized by means of the two separation streamlines in Fig. 8. It turns out that the larger of the two disturbance frequencies is more efficient for LSB control, because it produces earlier laminar-turbulent transition and a smaller bubble.

D. Effect of Increasing Disturbance Amplitudes

The disturbance amplitudes v' of the fundamental mode (1/0) $\beta = 5$ have been successively increased to find the relation between bubble size and forcing amplitude and to see whether the bubble can

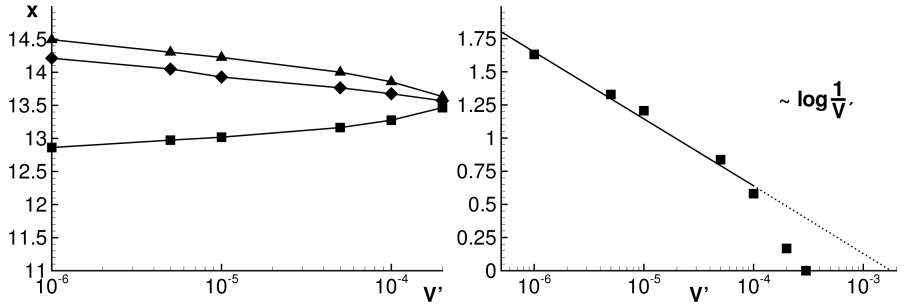

Fig. 10 Evolution of separation position (■), laminar-turbulent transition (◆), and reattachment position (▲) with disturbance amplitude v' (left); evolution of bubble length (right).

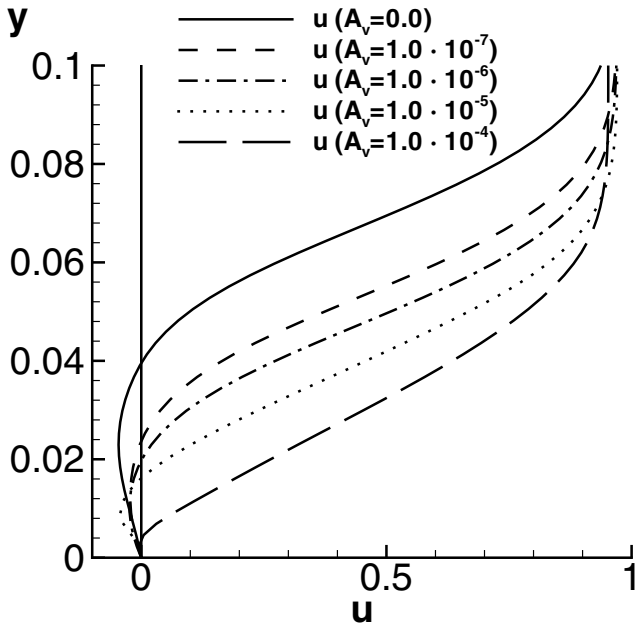

Fig. 11 Mean-flow velocity profiles at $x = 13.85$ for the cases with different forcing amplitudes.

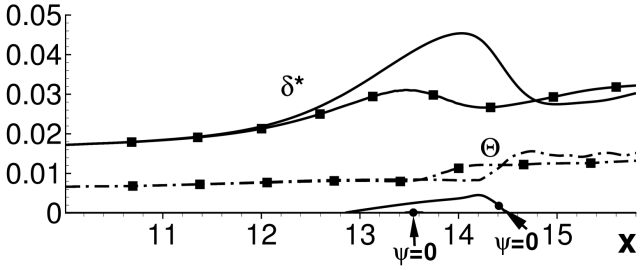

Fig. 12 Influence of forcing amplitudes ($v' = 10^{-6}$ and $v' = 2 \times 10^{-4}$, no symbols and symbols, respectively) on displacement and momentum thickness (solid and dash–dotted lines, respectively).

be made to completely disappear in the limit. The corresponding bubbles are compared in Fig. 9. Indeed, there is a continuous reduction in bubble height, a downstream shift of S, and an upstream shift of R as the forcing amplitude is increased from 10^{-6} to 2×10^{-4}.

Since the instability of the base-flow decreases, once the size of the LSB gets smaller, the additional energy input to influence the LSB increases in a nonlinear manner. Initially, the relation between bubble size and forcing amplitude is exponential as can be seen from an evaluation of the separation-, transition-, and reattachment-point positions versus forcing amplitude v', as well as the bubble length in Fig. 10.

The differences between the various cases are quite dramatic as illustrated in Fig. 11 by a comparison of the streamwise velocity profiles near the reattachment position of the smallest bubble. The profile of the unforced case is shown as a solid line.

Integral boundary layer parameters of the cases with smallest and largest forcing, that is, largest bubble and no bubble, are compared in Fig. 12. There is a threefold increase of displacement thickness over the bubble and a twofold increase of momentum thickness. When the bubble is suppressed both parameters increase to a lesser extent. Since a larger momentum thickness is indicative of more drag according to von Karman's integral momentum equation, it turns out that reducing the LSB must lead to a drag reduction.

E. Effects of Three-Dimensional Forcing

Since 3-D disturbances can be generated much easier in practice than perfect 2-D ones, one has to consider the efficiency of using 3-D disturbances for laminar separation bubble control, as well. Linear stability shows that oblique waves are nearly as amplified as two-dimensional ones for obliqueness angles smaller than about 30 deg [10]. This is illustrated in Fig. 13 by adding a 3-D forcing to the fundamental 2-D case from the previous figures. Using a 10-times larger forcing level $v' = 10^{-5}$ compared with the 2-D fundamental, which is now denoted by $(1/0)$ in the frequency spanwise wave number spectrum (h/k), displaces the 3-D mode $(1/1)$ above the 2-D one such that its almost identical growth compared with the 2-D one is easier to observe. Here, the fundamental spanwise wave number k is set to 5.4596 which corresponds to a spanwise wavelength of $\lambda_z = 1.15$ and an angle of obliqueness of $\phi = 20$ deg relative to the freestream direction. Adding this disturbance is equivalent to adding a pair of oblique waves $(1/\pm 1)$ because of spanwise symmetry imposed by the Fourier ansatz in z. To check the influence of the spanwise resolution the discrete Fourier series used to discretize the spanwise direction was truncated at $k = 9$ and $k = 19$, but this had no remarkable influence on the disturbance development inside the laminar separation bubble.

Because mode $(1/1)$ dominates in Fig. 13 the 3-D higher harmonics grow to large levels and turbulence sets in much earlier now with according consequences on the separation bubble and its

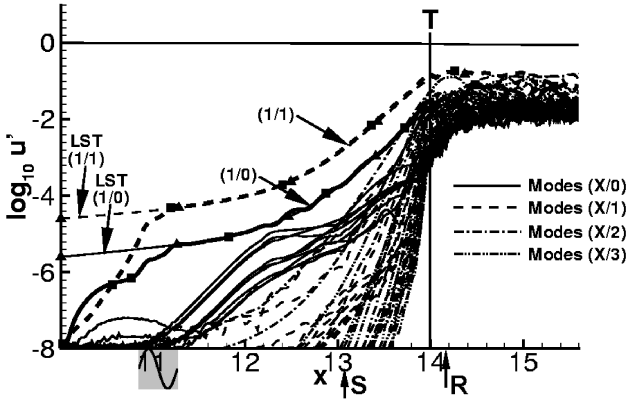

Fig. 13 Disturbance amplification for increased 3-D forcing at $v' = 10^{-5}$, $\beta = 5$.

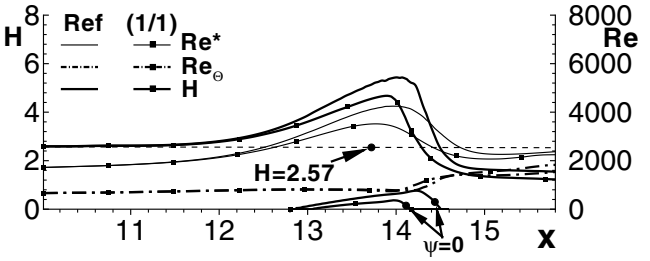

Fig. 14 Comparison of boundary-layer parameters for increased 3-D forcing (1/1) with 2-D forcing (reference case).

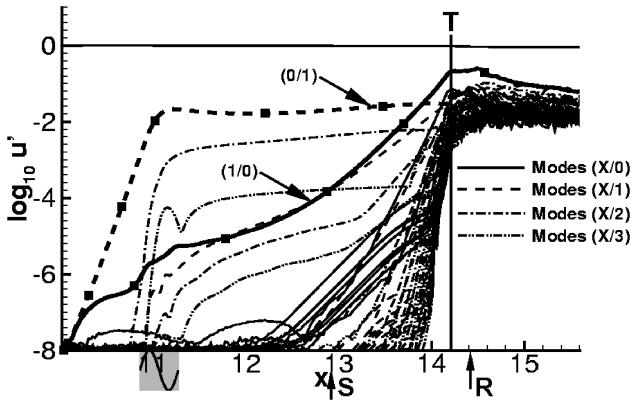

Fig. 15 Disturbance amplification under the influence of a steady 3-D disturbance (0/1).

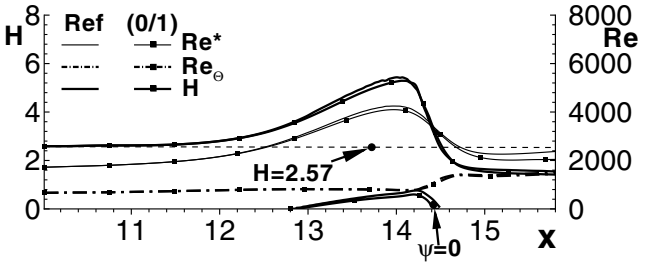

Fig. 16 Comparison of boundary-layer parameters for large-amplitude steady 3-D forcing (0/1) with the 2-D reference case (reference case).

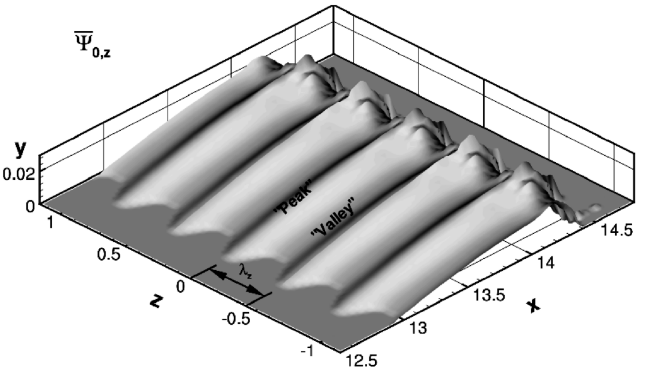

Fig. 17 Separation stream surface in case of large-amplitude steady 3-D forcing.

boundary-layer parameters. These latter are illustrated in Fig. 14 by comparing the case with increased 3-D forcing (1/1), identified with symbols, with the reference case from above.

The reaction of the flow to the 10 times larger oblique waves is comparable to a 10-fold increase of the 2-D forcing: The length of the laminar separation bubble decreases accordingly, and so does its height. Shape parameters and Reynolds numbers show a similar difference. Because of a nearly identical growth of the 3-D disturbance (1/1) in comparison with the 2-D (1/0) the laminar separation bubble can be controlled by either of the two at practically the same efficiency. However, downstream of the bubble the full 3-D case delivers a flow that resembles a fully turbulent boundary layer better than in the 2-D forced case, because of a lower shape factor.

F. Steady vs Unsteady Three-Dimensional Forcing

The next investigation will now show the effect of using a *steady* 3-D forcing to control the bubble. Such an approach is closer to "more traditional" techniques such as applying a row of small bumps upstream of separation that cause turbulence in order to prevent laminar separation. For this investigation the spanwise wave number has been increased to 15 which corresponds to a spanwise wave length of 0.4189 in the present scaling. To simulate such a steady 3-D "roughness," mode (0/1) has been forced with $v' = 10^{-3}$ in addition to the other modes in the reference case from above.

The resulting disturbance growth of individual modes is shown in Fig. 15. Initially, the spectrum is dominated by the steady 3-D mode and its higher harmonics (0/k), but in contrast to the traveling ones, these are only moderately amplified. More on the amplification of steady modes in a flow with LSB can be found in [23].

Apparently, the laminar-turbulent transition process is not much affected by the additional steady disturbance, despite its large initial amplitude. This can be explained by the fact that adding a steady roughness does not directly produce turbulence (which is inherently unsteady). The latter can occur only when wall roughness interacts with fluctuations of the freestream. Hence, in practice, large roughness is needed to cause laminar-turbulent transition via some bypass mechanism, that is, one without linear amplification of disturbances (in contrast to the driving mechanism in the present investigations).

In accordance with the above discussion the boundary-layer parameters in Fig. 16 show that the effect of the steady 3-D forcing is decent, despite the 1000-fold larger amplitude compared with the 2-D unsteady forcing above. The bubble shapes and the evolution of Reynolds numbers and shape factors remain practically unaltered.

A visualization of the 3-D separation surface (i.e., an approximation of the surface that separates the time-averaged recirculating flow inside the bubble from the external stream) shows that the steady 3-D disturbance amplitude was indeed considerably large such that it causes longitudinal grooves in the bubble (Fig. 17). Its inefficiency is hence not caused by a too small amplitude.

V. Conclusions

The above results show the advantages of the excitation of unsteady 2-D or 3-D disturbances with respect to "more traditional" approaches which rely on steady forcing. The basic idea is to provide optimal initial disturbances for laminar-turbulent transition, that is, instability waves which are most amplified. Larger initial amplitudes lead to an earlier laminar-turbulent transition and hence an earlier reattachment of the boundary layer. At the same time laminar separation moves downstream because the laminar separation bubble becomes shallower such that it has less upstream influence on the flow. Two-dimensional forcing generates instability waves that lead to time-periodic spanwise vortices after amplification and nonlinear saturation. These vortices enhance the wall-normal energy transfer already before the appearance of (3-D) turbulence. Using weakly oblique instability waves instead of two-dimensional ones it is observed that these grow approximately as fast as in the previous case (as long as the obliqueness angle is not larger than 30°) but now 3-D turbulence sets in much faster. Despite the qualitatively different mixing in both cases (due to turbulence in the latter in contrast to 2-D vortices in the first case) the net effect on the bubble size is the same, that is, the bubble shrinks.

Comparing unsteady forcing with a steady 3-D forcing that mimics 3-D roughness elements, it turns out that the latter are not

efficient as long as they do not cause a bypass transition. The scientific reason is that turbulence needs fluctuations (of a very specific frequency) which cannot be provided by steady roughness. Since separation can occur only under the influence of an *adverse* pressure gradient, the upstream region of favorable pressure gradient is not important for the viability of the present approach, regardless of its strength. A strong accelerating boundary layer followed by a strong deceleration is harmful only in so far as the usable distance between actuator and laminar separation bubble shrinks to a small value. The optimal position for the forcing of instability waves is always the position where these start to grow according to linear stability theory.

In summary, it has been shown that separation bubbles can be significantly reduced in size and finally removed very economically by low-amplitude boundary-layer disturbances, at least for the aerodynamic configurations investigated so far. The present findings seem to be fully in line with an experimental investigation of active control of flow over a sphere where it has been shown that the most efficient forcing frequencies are related to the instability properties of the adverse-pressure-gradient boundary layer before separation [24]. Because of a good agreement of boundary-layer parameters with those found in low-pressure turbines, and because of the excellent reproduction of such flows in a flat-plate boundary layer [8], it is expected that the present concept is equally valid in a turbo machine environment as in the laminar flow airfoil context, where it was initially intended. However, additional practical issues have to be considered if the present results are to be applied to a compressor or turbine. Mainly, the flow would be highly unsteady such that the laminar separation bubble periodically appears and disappears [8]. Turbulent wakes from upstream are known to have a comparable influence on the laminar separation bubble since they also move laminar-turbulent transition, however, in an uncontrolled manner. It remains to be investigated if an active control of those laminar separation bubbles which appear between two wake passages would further diminish the pressure losses or help to reduce the number of necessary blades. Another interesting problem would be to see if the present method is sufficiently strong to prevent an "open separation," that is, one where the boundary layer does not reattach after transition. As already mentioned above, our method works for higher pressure gradients (base flows *B* and *C*) equally well, but one might argue that these were not yet large enough to cause an open separation.

Acknowledgment

We thank the Deutsche Forschungsgemeinschaft (DFG), Bonn Bad Godesberg for financial support from Grant RI 680/11.

References

[1] Kerho, M., Hutcherson, S., Blackwelder, R. F., and Liebeck, R. H., "Vortex Generators Used to Control Laminar Separation Bubbles," *Journal of Aircraft*, Vol. 30, No. 3, 1993, pp. 315–319.

[2] Seifert, A., Eliahu, S., Greenblatt, D., and Wygnanski, I., "Use of Piezoelectric Actuators for Airfoil Separation Control," *AIAA Journal*, Vol. 36, No. 8, 1998, pp. 1535–1537.

[3] Munday, D., Jacob, J., and Huang, G., "Active Flow Control of Separation on a Wing with Oscillatory Chamber," AIAA Paper 2002-0413, 2002.

[4] Greenblatt, D., and Wygnanski, I. J., "The Control of Flow Separation by Periodic Excitation," *Progress in Aerospace Sciences*, Vol. 36, No. 7, 2000, pp. 487–545.

[5] Sinha, S. K., "Flow Separation Control with Microflexural Wall Vibrations," *Journal of Aircraft*, Vol. 38, No. 3, 2001, pp. 496–503.

[6] Bons, J. P., Sondergaard, R., and Rivir, R. B., "Control of Low-Pressure Turbine Separation Using Vortex Generator Jets," AIAA Paper AIAA-99-0367, 1999.

[7] Bons, J. P., Sondergaard, R., and Rivir, R. B., "Turbine Separation Control Using Pulsed Vortex Generator Jets," *Journal of Turbomachinery*, Vol. 123, No. 2, 2001, pp. 198–206.

[8] Stieger, R. D., and Hodson, H. P., "Unsteady Dissipation Measurements on a Flat Pate Subject to Wake Passing," *Proceedings of the Institution of Mechanical Engineers Part A, Journal of Power Engineering*, Vol. 217, No. 4, 2003, pp. 413–420.

[9] Dovgal, A. V., Kozlov, V. V., and Michalke, A., "Laminar Boundary Layer Separation: Instability and Associated Phenomena," *Progress in Aerospace Sciences*, Vol. 30, No. 1, 1994, pp. 61–94.

[10] Rist, U., "Zur Instabilität und Transition in Laminaren Ablöseblasen," Habilitation, Universität Stuttgart, Shaker Verlag, Aachen, 1999.

[11] Rist, U., "On Instabilities and Transition in Laminar Separation Bubbles," *Proceedings of the Confederation of European Aerospace Societies Aerospace Aerodynamics Research Conference* [CD-ROM], 2002.

[12] Rist, U., "Instability and Transition Mechanisms in Laminar Separation Bubbles," *Proceedings of Low Reynolds Number Aerodynamics on Aircraft Including Applications in Emerging Unmanned Aerial Vehicle Technology* [CD-ROM], VKI-LS, NATO Research and Technology Organization, Neuilly-sur-Seine, France, 2005.

[13] Augustin, K., "Zur Aktiven Beeinflussung von Laminaren Ablöseblasen Mittels Grenzschichtstörungen," Ph.D. Dissertation Universität Stuttgart, 2005.

[14] Rist, U., and Fasel, H., "Direct Numerical Simulation of Controlled Transition in a Flat-Plate Boundary Layer," *Journal of Fluid Mechanics*, Vol. 298, 1995, pp. 211–248.

[15] Kloker, M., Konzelmann, U., and Fasel, H., "Outflow Boundary Conditions for Spatial Navier–Stokes Numerical Simulations of Transition Boundary Layers," *AIAA Journal*, Vol. 31, No. 4, 1993, pp. 620–628.

[16] Kloker, M., "A Robust High-Resolution Split-Type Compact FD Scheme for Spatial Direct Numerical Simulations of Boundary Layer Transition," *Applied Scientific Research*, Vol. 59, No. 4, 1998, pp. 353–377.

[17] Rist, U., Maucher, U., and Wagner, S., "Direct Numerical Simulation of Some Fundamental Problems Related to Transition in Laminar Separation Bubbles," *Computational Methods in Applied Sciences: Proceedings of ECCOMAS '96*, John Wiley & Sons Ltd., Chichester, U.K., 1996, pp. 319–325.

[18] Maucher, U., Rist, U., and Wagner, S., "Refined Interaction Method for Direct Numerical Simulation of Transition in Separation Bubbles," *AIAA Journal*, Vol. 38, No. 8, 2000, pp. 1385–1393.

[19] Maucher, U., "Numerische Untersuchungen zur Transition in der laminaren Ablöseblase einer Tragflügelgrenzschicht," Ph.D. Dissertation, Universität Stuttgart, Shaker Verlag, Aachen, 2002.

[20] Augustin, K., Rist, U., and Wagner, S., "Active Control of a Laminar Separation Bubble," in *Aerodynamic Drag Reduction Technologies, Proceedings of the Confederation of European Aerospace Societies/ DragNet Conference*, edited by P. Thiede, NNFM 76, Springer–Verlag, Berlin, Heidelberg, 2001, pp. 297–303.

[21] Augustin, K., Rist, U., and Wagner, S., "Investigation of 2-D and 3-D Boundary Layer Disturbances for Active Control of Laminar Separation Bubbles," AIAA Paper 2003-0613, 2003.

[22] Reed, H., Saric, W. S., and Arnal, D., "Linear Stability Theory Applied to Boundary Layers," *Annual Review of Fluid Mechanics*, Vol. 28, 1996, pp. 389–428.

[23] Marxen, O., Rist, U., and Wagner, S., "Effect of Spanwise-Modulated Disturbances on Transition in a Separated Boundary Layer," *AIAA Journal*, Vol. 42, No. 8, 2004, pp. 937–944.

[24] Jeon, S., Choi, J., Jeon, W.-P., Choi, H., and Park, J., "Active Control of Flow over a Sphere for Drag Reduction at a Subcritical Reynolds Number," *Journal of Fluid Mechanics*, Vol. 517, 2004, pp. 113–129.

K. Fujii
Associate Editor